Journal of Basic and Environmental Sciences

ISSN
Online: 2356-6388
Print: 2536-9202

Research Paper Open Access

Studies on AC Electrical Conductivity and Dielectric Properties of Organic Acid-Doped PVA Solid Polymer Electrolyte Films

A. A. Eissa, E. M. Kamar, M. A. Mousa, M. Sameeh

Chemistry Department, Faculty of Science, Benha University, Benha, Egypt, 13511.

Corresponding author: A. A.Eissa (amany_aboueissa@yahoo.com)

Abstract:

In our research, we synthesized PVA/organic acid polymer electrolyte films using a solution casting technique. The resulting PVA films modified with acetic, oxalic, and citric acids were analyzed through XRD, FTIR spectroscopy, UV-Vis spectroscopy, SEM morphology analysis, stress-strain testing, and ac impedance measurements. The XRD analysis indicates that the introduction of organic acids into the PVA matrix enhances its amorphous nature. The IR spectra support the formation of polymer salt complexes. The findings revealed that the highest ionic conductivity at room temperature for the PVA/citric acid solid polymer membrane electrolyte system was 6.61×10^{-3} S cm $^{-1}$, while the ionic conductivity of pure PVA films was the lowest at **1.76×10^{-7} S cm^{-1}**. This study demonstrated that the increase in ionic conductivity was influenced by the type of organic acids used. The dielectric constant showed a significant exponential decline with rising frequency for both pure PVA and PVA films doped with organic acids. Additionally, the PVA/organic acid composite polymer membranes displayed favorable mechanical strength and ductility, making them an appropriate choice for polymer membrane electrolytes in energy storage application.

KEYWORDS: ionic conductivity, transport number, UV Visible spectra, PVA.

1. Introduction:

Lightweight, ultrathin, and flexible energy storage options are gaining attention to meet the present demands of portable and wearable electronics, such as smart phones, foldable displays, and solar panels.

Therefore, a flexible polymer electrolyte, such as gel polymer electrolyte that facilitate ion conduction, serves as an ideal choice for the fabrication and production of various energy storage systems [1–4]. In GPEs, the liquid electrolyte is contained within a polymeric matrix, minimizing the chance of leakage while exhibiting high conductivity at room temperature. The characteristics of polymer electrolytes are determined by the arrangement of the polymer network. Currently, various polymers including poly (ethylene oxide), poly (vinyl alcohol), poly (methyl methacrylate) , poly (acrylo nitrile), and poly (vinylidene fluoride) have been utilized in the production of GPEs.

PVA (polyvinyl alcohol) is a man-made biodegradable polymer. It has a high dielectric constant, is economical, and is safe for application. Known for its ability to form films and its chemical stability, it maintains adhesive properties and functional (OH) groups that offer considerable potential for chemical cross-linking [5]. PVA is an atactic semicrystalline polymer, with a carbon chain backbone featuring hydroxyl groups (OH) joined to the carbon, primarily comprised of 1,3-diol linkages [–CH2–CH(OH)–CH2–CH(OH)]. The functional groups enable PVA to form hydrogen bonds with compatible dopants [6]. Furthermore, PVA is notable for its polarity, adequate thermal stability , ease of processing, and transparence [7,8] .Other remarkable characteristics of PVA include its non-toxicity, water solubility, biodegradability, and compatibility with biological systems [9].

PVA can be readily created as a membrane. The semicrystalline characteristics of PVA film arise from the hydroxyl groups in PVA that absorb significant amounts of water, thereby boosting ionic conductivity [10-18]. The primary limitation of PVA is its conductivity, which can be enhanced using various methods to transform its semicrystalline phase into an amorphous state by incorporating suitable salts, plasticizers, nano-fillers, or by blending with other polymer hosts [19]. The polymer's high dielectric constant aids in the dissociation of the salt, while its low viscosity facilitates greater ionic mobility in the electrolyte, leading to an increased electrical conductivity value.

This paper presents the results from research that investigated the vibrational, electrical, dielectric, and optical properties of PVA films that have been doped with organic acids. The research aims to gain insights into charge transport mechanisms within polymer chains. Additionally, the

optical properties have been evaluated to determine the characteristics of the optical band gap and transparency. The electrolyte films generated have been examined using X-ray diffraction (XRD), Fourier transform infrared (FTIR) spectroscopy, UV-Vis spectroscopy, SEM morphology analysis, stress-strain testing and ac impedance spectroscopy. One of our objectives is to apply the developed membrane in the energy production devices.

2. Experimental

2.1. Materials

PVA (96.5% hydrolyzed, average Mw = 85,000–124,000) was acquired from Acros Organics (Geel, Belgium). Acetic, oxalic, and citric were provided from El Nasr Co. (Cairo; Egypt), and ethanol from Doummar & Sons Co. (Taufkirchen; Germany), All raw materials were used without further purification. Double-distilled water and ethanol have been used as solvents for the experiment.

2.2. Sample preparation

Various organic acid solutions (acetic, oxalic, citric) and unmodified PVA polymer electrolyte membranes were created. A quantity of 0.02 mol of each acid electrolyte was combined with 1g of PVA in 40 ml of deionized water, then stirred and heated at 90°C until a uniform viscous solution was formed. The resulting homogeneous mixtures were poured into clean petri dishes and air-dried in ambient conditions for two weeks to facilitate membrane formation. Once air-drying was complete, the samples were placed in a desiccator with silica gel to ensure complete dryness before further experimentation and characterization. The unmodified PVA membrane was produced using the previously described method without the incorporation of organic acids. The samples were designated as PVA, PVA-acet ,PVA-oxal, and PVA-citr, indicating the unmodified membrane along with those infused with acetic, oxalic, and citric acids, respectively.

2.3. Characterizations

The amorphous and crystalline characteristics of the synthesized samples were examined using an **XRD** diffractometer with Cu-Kα radiation (λ = 1.5405 Å) within the 2θ range of 10 to 80°. The Fourier transform infrared (FTIR) spectra were recorded with a SHIMADZU-IR Affinity-1 Spectrometer over a frequency range of 4000 to 400 cm^{-1}, utilizing a resolution of 1 cm^{-1} to investigate the interactions between the prepared PVA membrane and the incorporated materials. Morphological analysis was conducted using

a scanning electron microscope (JEOLJSM-6510LV, USA). The mechanical strength of the polymer electrolyte membranes was evaluated utilizing a rectangular shape film using Pack Test UTM model KC-3000 fitted with 500 N load cell. The membrane was shaped into a rectangle measuring 4 cm by 3 mm, and its thickness was measured with a micrometer. Subsequently , the membrane underwent testing with a gauge length set at 2 cm, a load cell rated for 10.000 cN, and a testing speed of 6 mm/min. The average of three repeated measurements was used to evaluate the sample's mechanical characteristics. The formulas listed below were applied to calculate the tensile strength Ts and the broken elongation E:

$$Ts = \frac{P}{bd} \qquad (1)$$

$$E = [(L - Lo)/Lo] \times 100 \qquad (2)$$

where P represents the load, b denotes the width of the sample, d indicates the thickness of the sample, L refers to the length of the sample after it has fractured, and L_o is the original length of the sample.

The ionic conductivity of the polymer electrolyte membranes was assessed using the Electrochemical Impedance Spectroscopy (EIS) technique. The membranes were cut into rectangular shapes measuring approximately 2 cm x 4 cm and then positioned between two stainless steel electrodes. Impedance data collection was conducted at room temperature across a frequency range of 100 Hz to 1 MHz at a voltage of 1 V using the Agilent LCR E4980 equipment. The analysis of the impedance data was performed with Zview® software to determine the membrane resistance value. The bulk resistance value (R_b) was determined from the high-frequency intercept on the real impedance axis of the Nyquist plot [20].

The following equation was used to determine the membrane's ionic conductivity:

$$\sigma = \frac{d}{RbA} \qquad (3)$$

where A indicates the membrane's region under examinations.

3. Results and discussion

3.1. XRD Analysis

The XRD patterns for both virgin PVA film and modified-PVA solid electrolyte films are presented in Fig. 1-a. The diffraction peaks for PVA are observed at 2θ values of 20.11° and 40.71°. The broad peak located at 2θ = 20.11° indicates that PVA exhibits a combination of amorphous and crystalline characteristics. This broad peak at 20.11° matches to a d-spacing of 4.4 Å and the reflection plane of

(101), highlighting the **semi-crystalline nature of PVA**. The absence of XRD peaks for the organic acids in the spectra of the doped PVA indicates that these acids have completely dissolved within the polymer matrix, which enhances the amorphous phase of the polymer. The reduced intensity of peaks related to unmodified PVA suggests a decrease in the crystallinity of the resulting electrolytes, implying that a combination of the additives and PVA has been achieved. It is important to note that in the amorphous region, mobile charge carriers have greater mobility than in the crystalline phase, since the amorphous arrangement provides more room for ion diffusion and permits segmental movement of the polymer chain, thereby enhancing ion hopping and resulting in improved ionic conductivity [21-23].

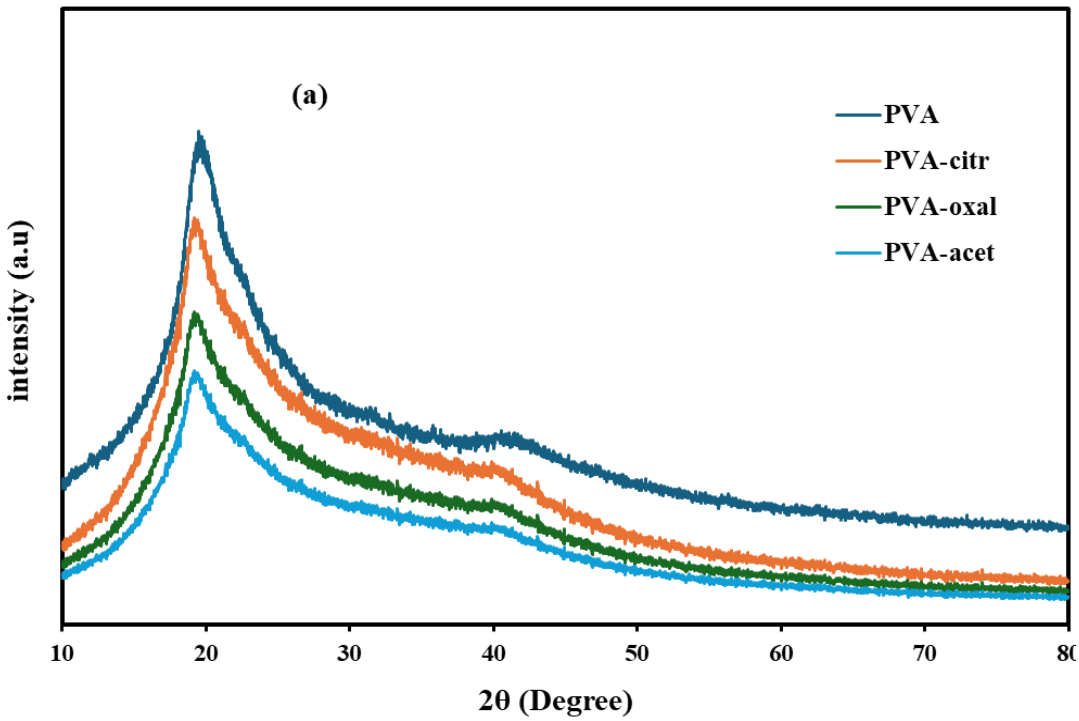

Fig. (1a): XRD of the investigated unmodified and modified PVA.

3.2. FTIR Studies

The FTIR analysis of the tested membrane was conducted to demonstrate the potential interactions between the introduced organic acids and the PVA chains. The findings are presented in Fig. 1-b. Considering the chemical structure of PVA, a broad peak around 3400 cm^{-1} is detected, which assigned to the O–H stretching from the intramolecular hydrogen bonds [24]. Additionally, peaks at 2920 cm^{-1} and 2840 cm^{-1} imply the symmetric and antisymmetric vibrations of the C-H bond

[25], while the peak at 1408 cm^{-1} represents the symmetric vibration of the C-H group [26]. The variations in peak intensities and the detected red-shift in the spectra of the modified PVA in contrast to pure PVA indicate possible interactions between the protons from organic acids and the polar groups (O-H and C-O) present in PVA [27] which indicated in Table 1. The H^+ ions can hop through each PVA chain's oxygen site, enhancing conductivity [28-30]. The spectra of the PVA-organic acid membranes also reveal vibration bands between 450 and 700 cm^{-1}, attributed to the deformation of the δ(COO) group.

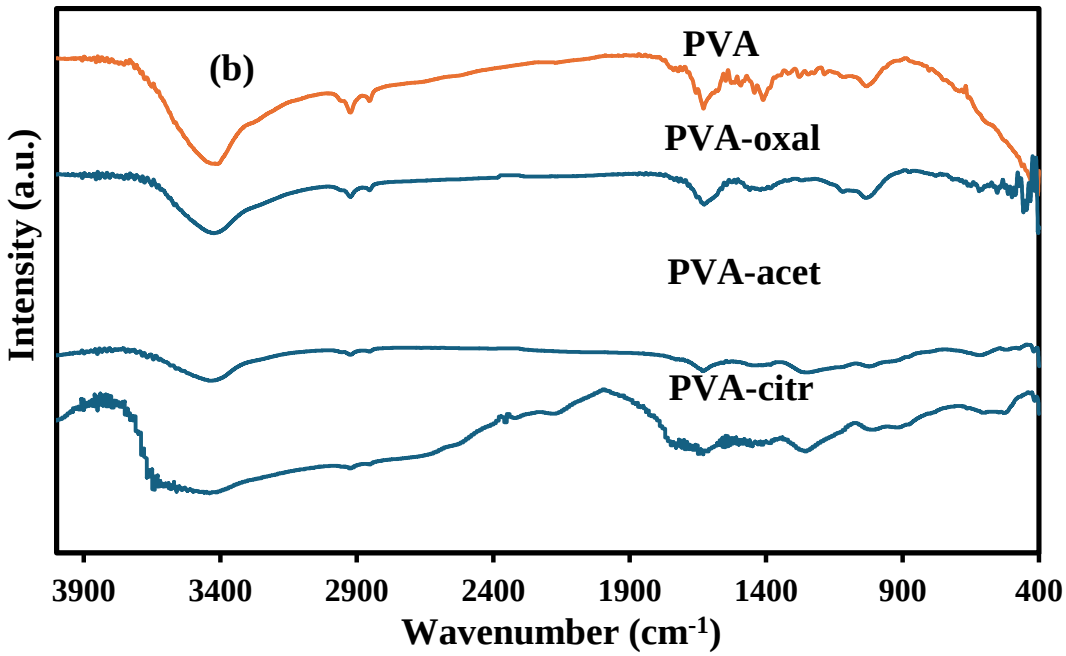

Fig. (1b): FT-IR of the investigated unmodified and modified PVA.

Table (1): FTIR peaks of PVA and its electrolyte membranes.

Band	Wave number (cm^{-1})			
	PVA	PVA-oxal	PVA-acet	PVA-citr
O-H stretching	3400	3411	3426	3440
C-H symmetric	1408	1420	1436	1450

3.3 Morphology Study

The surface structure of the PVA and electrolyte membranes was examined using scanning electron microscopy. Figure 2 displays the SEM images of both PVA and modified PVA electrolyte membranes. Incorporating additives into PVA creates multiple open voids that play a vital role in

ionic conductivity; a porous structure provides sufficient pathways for ion transport. As a result, these pores can hold water molecules, thus creating an effective pathway for ion conduction.

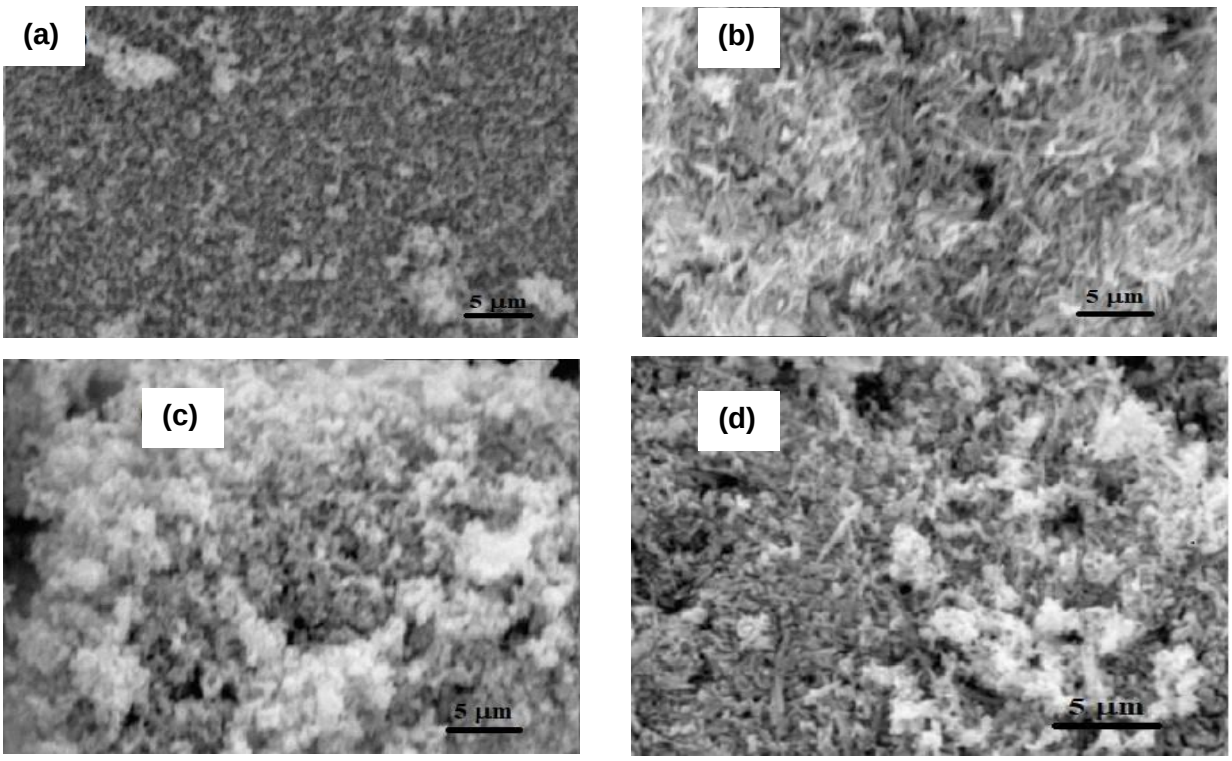

Fig. (2): SEM of unmodified PVA (a) and PVA-acet (b), PVA-oxal (c) and PVA-citr (d) electrolyte membranes.

3.4 Mechanical Study

The mechanical characteristics are considered crucial for evaluating the possible applicability of the examined membranes in Direct Methanol Fuel Cells (DMFCs). The tensile strength and percentage elongation at break for PVA and its electrolyte membranes were evaluated, with results presented in Table 2. PVA has demonstrated a significant tensile strength of 67.7± 5.1. In contrast, the electrolyte membranes exhibit reduced tensile strength and elastic modulus, attributed to the presence of more chains or shorter chains that form crystalline layers, which permit easier slipping under stress. In this context, the free ends of the chains serve as imperfections in the system, which reduces both mechanical strength and elastic modulus. The elongation at break of the electrolyte exceeds that of the pure PVA film because of the incorporation of organic acid. The incorporation of organic acid at the molecular level diminishes the

interactions among the polymer chains. At the same time, this process expands the free volume or spaces between the chains, improving the flexibility of the polymer chains [31,32] or gaps between chains, enhancing the flexibility of the polymer chains [31,32]. Additionally, organic acids have been shown to decrease the number of active centers within the polymer chains, leading to reduced intermolecular and intramolecular interaction [33].

Consequently, the stiffness of the host polymer decreases, resulting in a more flexible electrolyte film, which aligns with the outcomes of the characterization tests. Incorporating fillers reduced crystallinity, which in turn decreased the tensile strength values. Furthermore, the insufficient adhesion between the polymer matrix and the filler, coupled with increased constraints on the polymer segments, could lead to this reduction.

Table (2): Mechanical properties of PVA and its electrolyte membranes

Sample	Tensile Strength (MPa)	Elastic Modulus (GPa)	Elongation (%)
PVA	**67.7±5.1**	**0.645±0.025**	**11.3±0.7**
PVA-acet	**61.8±3.8**	**0.571±0.031**	**15.1±0.6**
PVA-oxal	**55.2±2.1**	**0.523±0.023**	**18.4±0.5**
PVA-citr	**51.1±3.5**	**0.481±0.027**	**21.1±0.7**

3.5 UV-vis Study

Figure 3 illustrates the UV-visible spectrum of the analyzed membranes. No absorption peaks were detected in the visible area of the UV-visible spectrum (i.e., beyond 380 nm), indicating that the membranes maintained high transparency. Therefore, the films produced may be appropriate for constructing electrochromic devices where transparent electrolytes are needed [34]. Pure PVA's spectrum shows a prominent absorption peak at 228 nm, which is ascribed to the n→π* transition, and two smaller absorption bands at 305 and 350 nm, which are associated with the C=O group and the π→π* transition, respectively. These bands are caused by unsaturated bonds present in the polymer's tail-head, like C=O and/or C=C. Table 3. indicate the notable peak at 228 nm has shifted to a lower wavelength in the solid electrolyte. This blue shift could result from reduced hydrogen bonding between PVA chains and the polar carboxylate groups of organic acids. Such a shift in wavelength influences the band structure and band gaps, resulting in a change in the absorption edge.

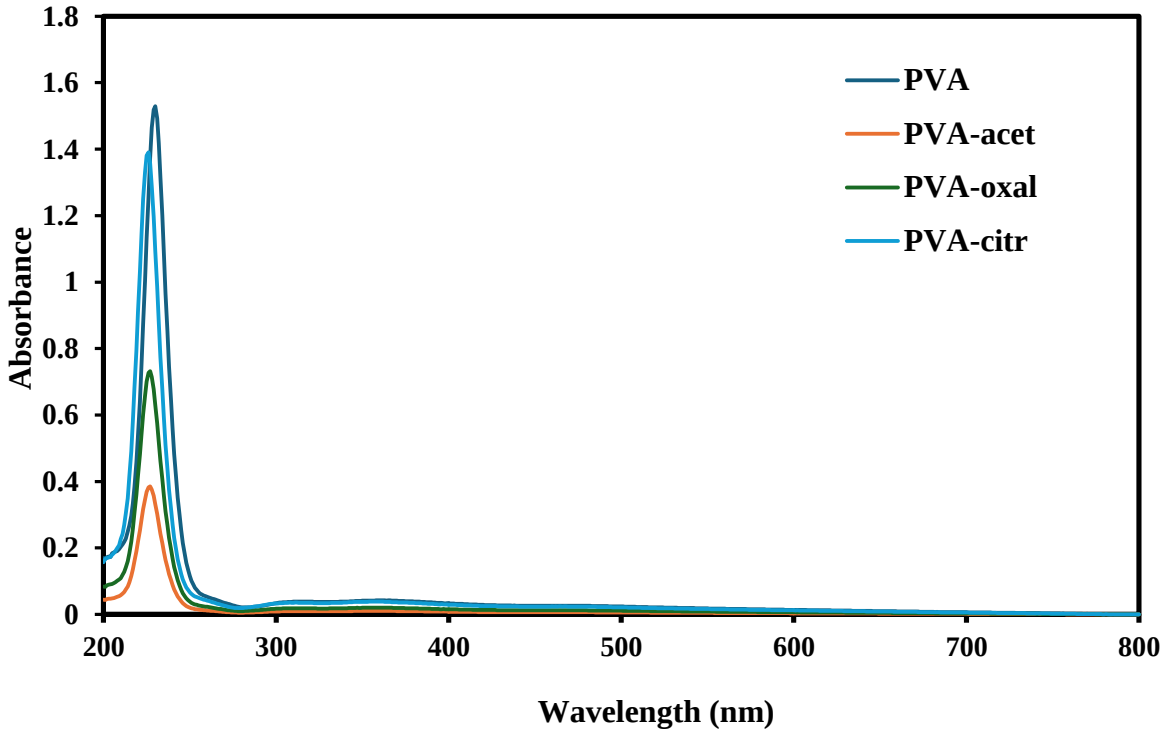

Fig. (3:) UV-vis spectra of the investigated membranes.

Table 3: UV-Visible spectra of PVA and its electrolyte membranes.

Samples	Wavelength (nm)
PVA	**228**
PVA-oxal	**227**
PVA-acet	**226**
PVA-citr	**225**

3.6. Impedance and ion transport study

Electrochemical impedance spectroscopy (EIS) is commonly employed to investigate the responses of samples (semicircle and spike) in both high- and low-frequency areas. These response areas relate to ion conduction in the electrolyte's bulk and electrode polarization's effects, respectively [35]. In this study, Figs. 4a-d present the Nyquist plots of the evaluated films. The plots of organic acid doped PVA (4b-d) reveal two distinct regions: (1) a semicircle in the high-frequency domain and (2) a slanted line in the low-frequency domain. The semicircle indicates the electrolyte's bulk characteristics, while the slanted line corresponds to blocking electrodes. The point at which the semicircle

ends and the inclined area begins is referred to as the bulk resistance of the material. According to Figs. (4 b-d), it is clear that all the altered PVA films show a significant decrease in the diameter of the high-frequency semicircle, i.e., a decrease in the bulk resistance with incorporating the organic acids into PVA. By utilizing z-fit software to analyze the impedance data, accurate bulk resistance (R_b) values were determined in Table 4.

Table (4) :Values of bulk resistance (R_b) of the investigated membranes.

Samples	Bulk resistance (Ω)
PVA-acet	**195**
PVA-oxal	**19.5**
PVA-citr	**9.75**

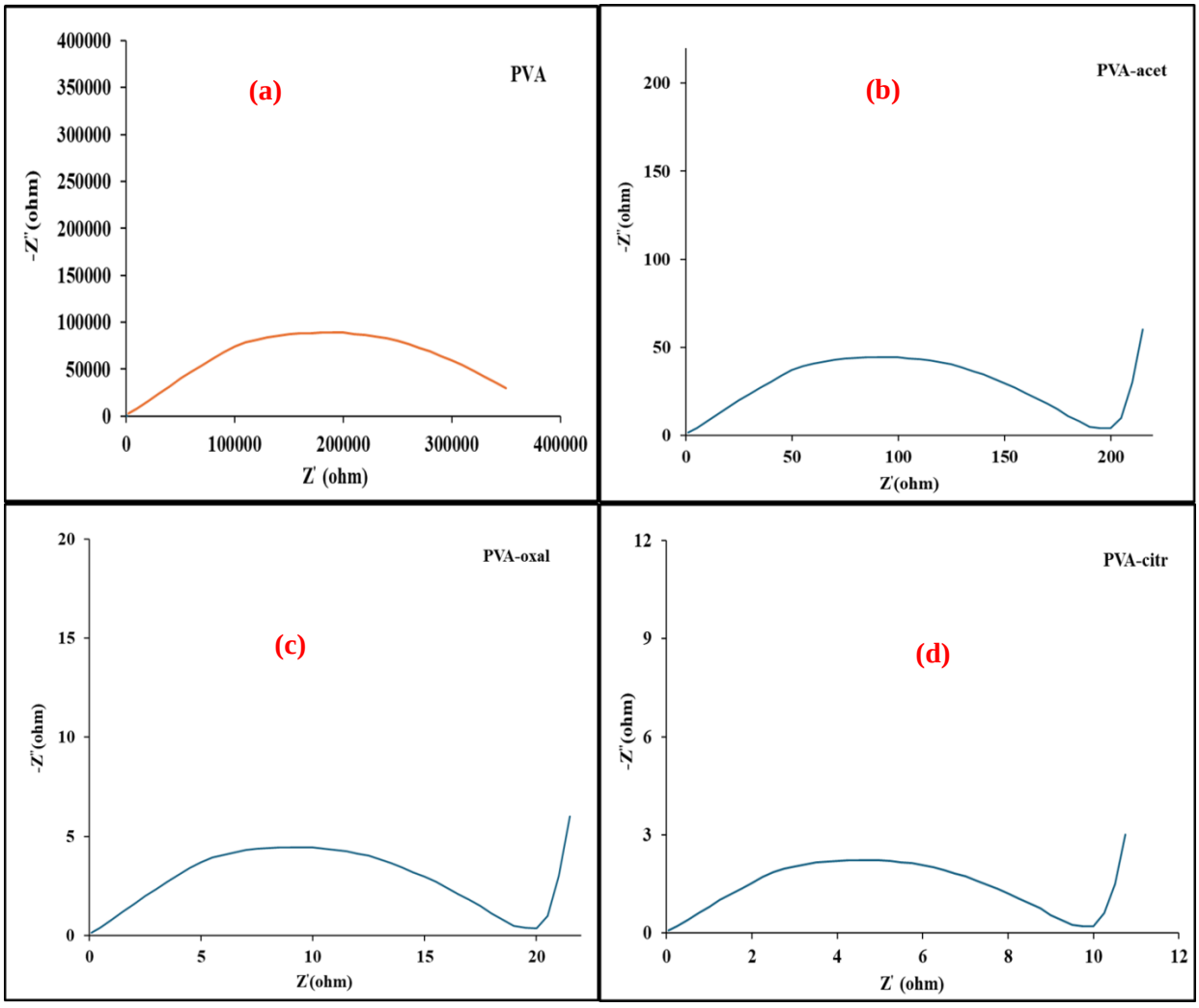

Fig. (4): EIS of the investigated unmodified and modified PVA membranes.

The equation was utilized to calculate the ionic conductivity. The values of conductivity obtained from calculations are presented in Table 4. The Table indicates that the bulk resistance value decreases or the conductivity value increases when organic acids are added to the PVA matrix in the order: PVA-citr > PVA-oxal > PVA-acet > PVA. This improvement is attributed to the increased concentration of charge carriers resulting from the transition from a semi-crystalline structure to an amorphous one. Additionally, incorporating organic acids into PVA facilitates the mobility of charge carriers by disrupting their arrangement. Marf et al. [36] have shown the electrolytes' ionic conductivity dependency on the flexibility of the polymer chain and how much of ion mobility.

Table (5): Ionic conductivity of the investigated membranes.

Sample	**σ_{ion} (S cm^{-1})**
PVA	**1.76x10^{-7}**
PVA-acet	**3.42x10^{-4}**
PVA-oxal	**3.24X10^{-3}**
PVA-citr	**6.61x10^{-3}**

3.7. Dielectric studies

Dielectric analysis is a useful approach for learning about the conduction mechanisms in electrolyte polymer membranes as well as the interactions between ions and polymers. When an electric field is applied, dielectric materials become electrically polarized based on the principle of polarization. A solid material's dielectric response may be defined by expressing the relative dielectric constant as a complex number with real and imaginary components: $\varepsilon^* = \varepsilon' + j\,\varepsilon''$. In this expression, ε' and ε'' denote the real and imaginary parts of the dielectric constant, respectively, which indicate the energy stored in the dielectric material due to polarization and the energy loss occurring while an electric field is applied [37,38].

The following relation were used to get the real component of the dielectric constant (ε') from complex impedance data:

$$\varepsilon' = -[Z''/\omega C_o(Z''^2 + Z'^2)] \qquad (4)$$

The following equation provides the imaginary component of the dielectric constant (ε'')

$$\varepsilon'' = [Z'/\omega C_o(Z''^2 + Z'^2)] \qquad (5)$$

In this context, Z' represents the real component of the impedance, Z'' denotes the imaginary component of the impedance, ω

signifies the angular frequency, and C_o indicates the geometrical capacitance. The evaluated dielectric constant and dielectric loss as function of the applied ac-frequency are illustrated in Figs. 5a, b. The results indicate that the dielectric constant increases with the incorporation of organic acids into pure PVA, following the order PVA-citr > PVA-oxal > PVA-acet > PVA. Moreover, there is a significant variation in the dielectric constant with changes in frequency, showing a decrease in the dielectric constant as frequency rises. This phenomenon can arise due to ionic and electronic polarization, influenced by the significant immobilization of ions and space charge polarization. This leads to a reduced number of dipoles available to align with the electric field. The drastic drop in dielectric constant is evident across a frequency range of 1 to 100 kHz, as charge carriers do not have sufficient time to align with the direction of the field. At very high frequencies, the rapid oscillation of the field leads to the observed frequency-independent ε′ behavior [39,40]. Ions can migrate in the electric field direction; however, at low frequencies, the blocking electrodes prevent them from reaching the external circuit, causing a dispersion characterized by elevated ε′ values. Consequently, ions get trapped at the interface between the electrode and electrolyte, creating a layer of electrode polarization [41,42]. This suggests electrode polarization and space charge impacts dominate the low-frequency zone. The stored charge rises, enhancing ionic conductivity.

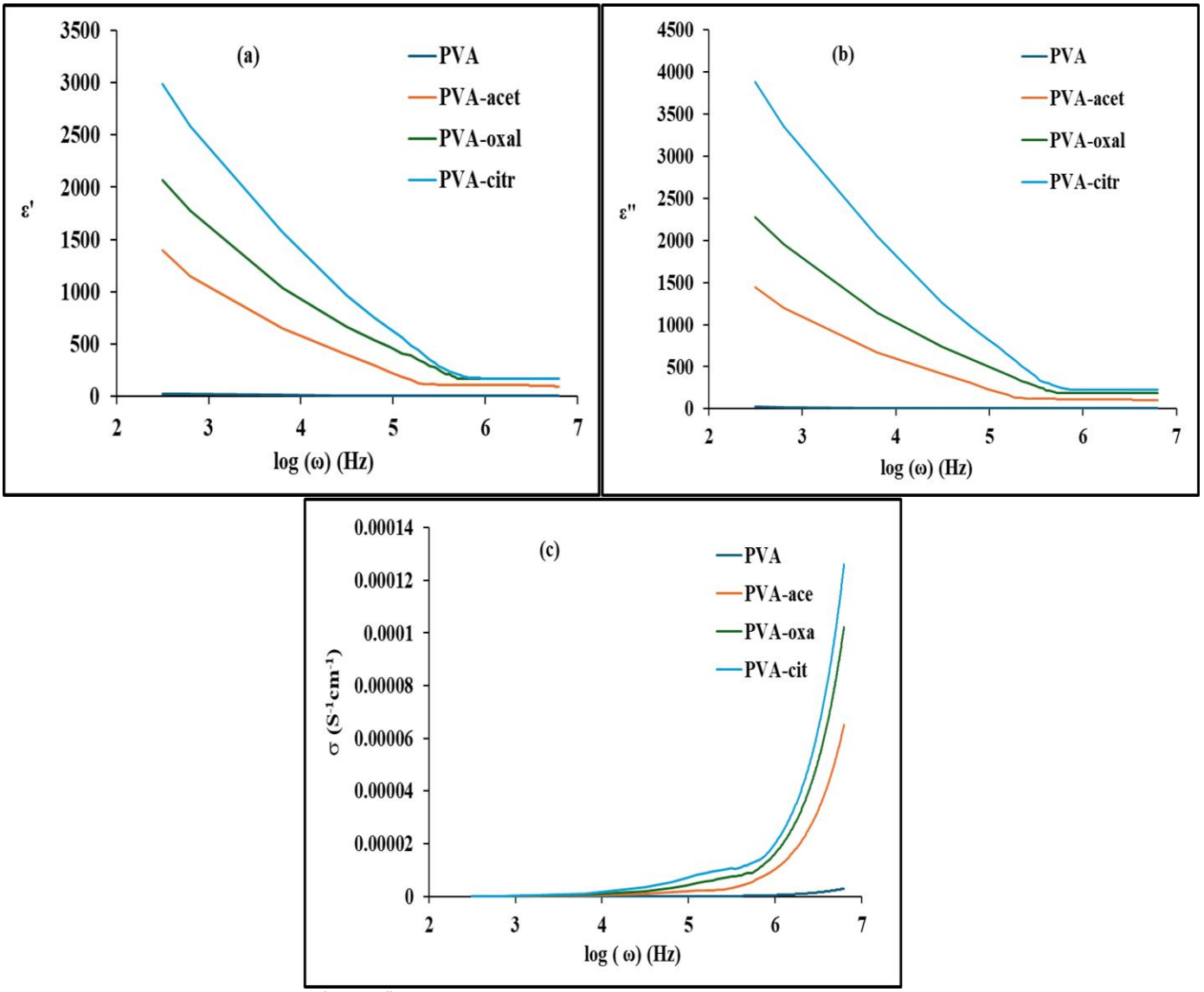

Fig. (5): The variation of ε'(a) , ε'' (b) and σ_{ac} (c) versus frequency for all investigated samples.

The dielectric loss (ε") can be utilized to assess the intensity and frequency of relaxation based on the distinctive characteristics of dipolar relaxation. The frequency-dependent dielectric loss are illustrated in Fig. 5(b). It has been noted that for every membrane tested, ε" exhibits a decline as frequency increases. Furthermore, adding organic acids resulted in a stronger bulk relaxation, which increased dielectric loss. The rise in conductivity influences the value of ε", promoting a higher dielectric constant, ε". This indicates that high values of dielectric loss ε" signify an improvement in the motion of free charge carriers within the membrane.

3.8. AC Conductivity Studies

The formula listed below was applied to find out the ac-conductivity of the

membranes under study based on the dielectric constant.

$$\sigma_{ac} = \varepsilon_o \omega \varepsilon'' \quad (6)$$

, where ε_o being the permittivity of free space. The variation of AC conductivity with frequency for both virgin PVA and modified PVA polymer electrolyte is illustrated in Figure **5c**. As seen in Figure **5c**, conductivity rises with the increase in frequency. The PVA-acet membrane showed the highest conductivity among the membranes. The increase in AC conductivity is due to increase in the number of carboxylic acids (citric >oxalic > acetic) in polymer matrix resulting in relatively more number of free ions. Consequently, there is a rise in mobile charge carriers, as indicated in Table 6. Moreover, due to the increased amorphous regions in the modified PVA compared to virgin PVA, the charge carriers can move more freely within the amorphous polymer matrix, leading to enhanced conductivity. Generally, as the degree of crystallinity diminishes, conductivity tends to increase, which aligns with the observed enhancement in the amorphous nature [43].

Table 6. Charge carrier mobility of the investigated membranes

Samples	Charge carrier mobility (μ)
PVA-acet	**2.14×10^{15}**
PVA-oxal	**1×10^{16}**
PVA-citr	**1.38×10^{16}**

3.9.Transference number measurement (TNM)

The TNM method assesses the primary charge carrier species within the polymer electrolyte. Observing the current plot over time (refer to Fig. 6 (a,b,c)), it is evident that the current diminishes until a consistent state is achieved when a voltage of 0.2 V is applied. This figure illustrates the polarization current over time for the relatively high-conductivity electrolyte. The elevated original current value is attributed to the involvement of both charge carriers—electrons and ions—during the initial phase. Additionally, a significant reduction in current is observed before reaching a steady state. It is essential to keep in mind that electrons can go through stainless steel electrodes because of the ionic barrier they create [35]. Having a t_{ion} value close to one is crucial, representing an ideal scenario which indicated in Table 7.

Table 7: TNM of the investigated membranes.

Sample	t_{ion}	t_e
PVA-acet	**0.992**	**0.008**
PVA-oxal	**0.993**	**0.007**
PVA-citr	**0.996**	**0.004**

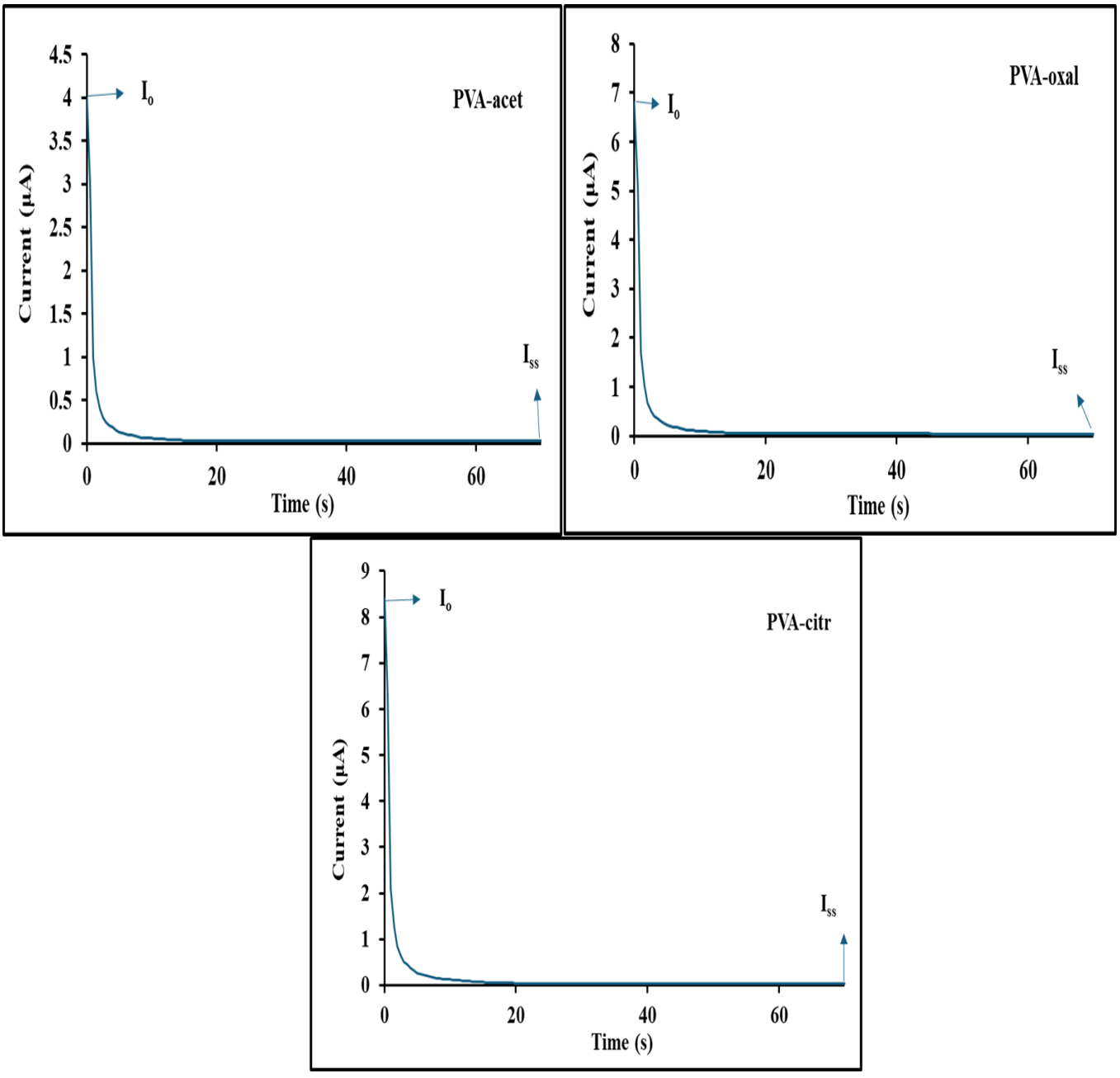

Fig. (6): Plot of current vs. time for modified PVA membrane under voltage of 0.2 V.

3.10. Electrical modulus analysis

Electrical modulus was employed to investigate the electrical relaxation mechanisms in ion-conducting materials and can offer deeper insights into the polarization suppression effect inside the system [44]. The key benefit of this approach is that it minimizes the effects of electrode polarization. One way to represent the electrical modulus is with the relation [45]:

$$M" = M' + jM" \quad (7)$$

The real ($M^{'}$) and imaginary ($M^{''}$) parts of the complex electrical modulus were evaluated employing the next expressions:

$$M' = - \omega Co\, Z" \quad (8)$$

and

$$M" = \omega\, Co\, Z' . \quad (9)$$

Figure 7 illustrates how the electric modulus ($M^{'}$) 's real part varies with frequency at room temperature. It was found that at low frequencies, $M^{'}$ approaches zero, suggesting that electrode polarization contributes very little [46]. The extended tail observed at low frequencies indicates the capacitive trend of the electrolytes, where significant electrode polarization happens without dispersion [47, 48] The observed dispersion of $M^{'}$ at higher frequencies is due to the relaxation conductivity.

Figure (7b) reveals that the unmodified PVA experiences a relaxation peak at high frequencies, while PVA films with added organic acids exhibit a prolonged tail at low frequencies that increases at higher frequencies. The extended tail and very low $M^{''}$ value result from the significant capacitance linked to the electrode polarization effect, indicating that charge carriers accumulate due to the large electrode/electrolyte interface. The absence of $M^{''}$ peak in the organic acid-modified films is attributed to the limitations of the experimental frequency. The rise in higher frequency ranges is linked to the long-range hopping of charge carriers. Thus, it can be said that ion transport in PVA electrolytes treated with organic acid happens by long-range hopping of charge carriers [49].

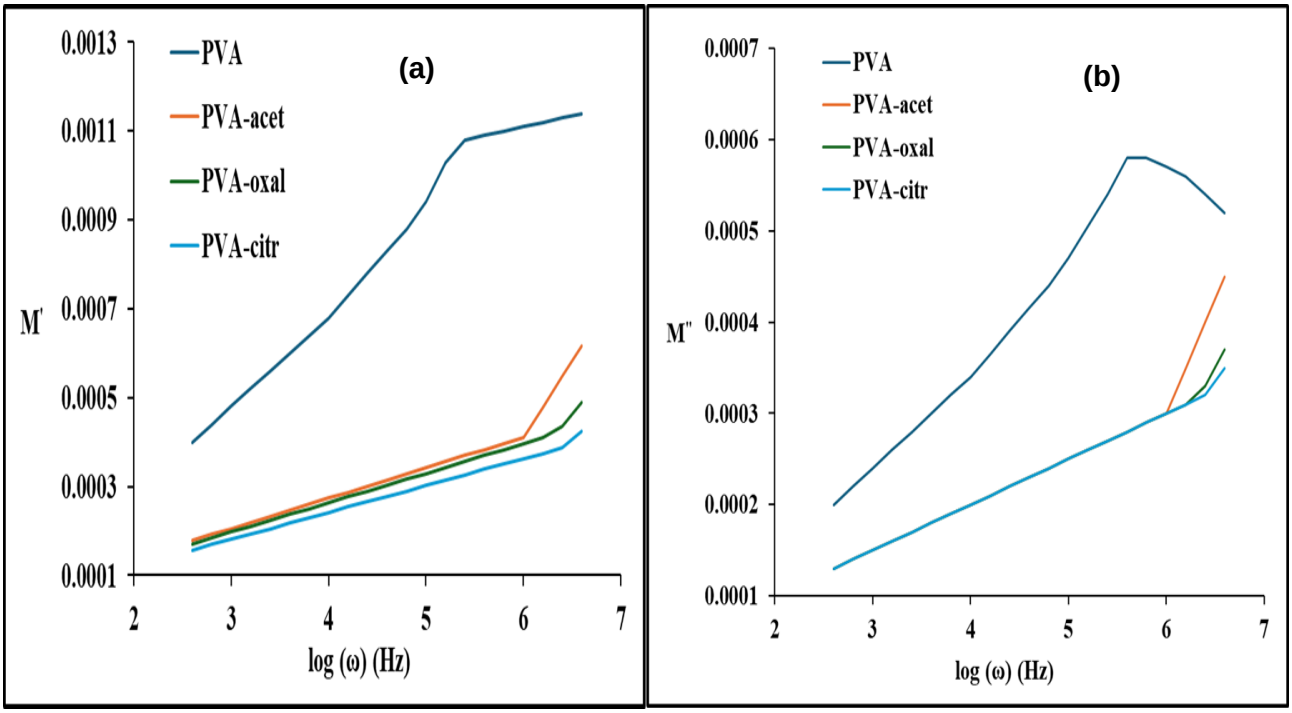

Fig. 7. The variation of M'(a) , and M" (b) versus frequency for all investigated samples.

4. Conclusions

Polymer electrolyte films based on PVA have been created with the addition of organic acids (acetic, oxalic, or citric) using the solution casting method. The XRD analysis of investigated samples shows a broad peak at roughly 20.11˚ for pure PVA, which shifts in the samples modified with PVA. Additionally, the intensity of this peak diminishes while the full width at half maximum increases, indicating an amorphous character of the complexed system. The absence of peaks associated with organic acids in the modified PVA suggests that the organic acids have completely dissociated within the polymer matrix. Therefore, XRD analysis confirms the formation of a complex between the polymer and the organic acids. FTIR analysis of both pure PVA and PVA incorporated with organic acids indicates the establishment of interactions between the functional groups of PVA and those of the organic acids. The strength and ductility of PVA enhance with the incorporation of organic acids. and AC conductivity measurements reveal that for both pure PVA and PVA composites doped with organic acids, the AC conductivity increases as the frequency rises. This may be attributed to the enhanced mobility of charge carriers within the composite film. The investigation highlighted significant

molecular dipolar polarization at elevated radio frequencies, along with a frequency-dependent dielectric permittivity mainly affected by interfacial polarization at lower frequencies. Modified PVA with organic acids demonstrates high ionic conductivity, following the order of PVA-citr > PVA-oxal > PVA-acet. Specifically, PVA-citr exhibits an ionic conductivity of up to 6.61×10^{-3} S cm^{-1} at room temperature, whereas pure PVA films display the lowest ionic conductivity of $\mathbf{1.76 \times 10^{-7}}$ S/cm.

5. References:

[1] Q. Li, J. Chen, L. Fan, X. Kong, Y. Lu, Progress in electrolytes for rechargeable Li-based batteries and beyond, Green Energy Environ,vol.1, pp 18–42 , 2016.

[2] X. Cheng, J. Pan, Y. Zhao, M. Liao, H. Peng, Gel Polymer Electrolytes for Electrochemical Energy Storage, Adv. Energy Mater ,vol.8, pp. 1702184, 2018.

[3] X. Feng, M. Ouyang, X. Liu, L. Lu, Y. Xia, X. He, Thermal runaway mechanism of lithium-ion battery for electric vehicles, Energy Storage Mater ,vol.10 , pp. 246–267,2018.

[4] Y. T. Tleukenov, G.Kalimuldina, A.Arinova, N.Issatayev, Z.Bakenov, A.Nurpeissova., Polyacrylonitrile-Polyvinyl Alcohol-Based Composite Gel-Polymer for All-Solid-State Lithium-Ion Batteries, polymers, vol. 14, pp 5327, 2022.

[5] K. Li, L.Xiaorui, L. Chunyan, Y. Shen, D. Wan, Cross-linked polyvinyl alcohol modified by aziridine cross-linker for effective paper sizing, Progress in Organic Coatings,vol. 161, pp. 106482 ,2021.

[6] S. B. Aziz, Modifying poly (vinyl alcohol)(PVA) from insulator to small-band gap polymer: A novel approach for organic solar cells and optoelectronic devices, J. Electron. Mater,vol. 45, pp. 736–745 , 2016.

[7] S. B. Aziz, M.H.Hamsan,Wrya O.Karim, Ayub Sh.Marif, Rebar T.Abdulwahid, M.F.Z.Kadir, M.A.Brza, Study of impedance and solid-state double-layer capacitor behavior of proton (H+)-conducting polymer blend electrolyte-based CS:PS polymers, , Ionics, vol. 26 , pp. 1–15 , 2020.

[8] S. B. Aziz, , M.H.Hamsan , M.A.Brza , M.F.Z.Kadir ,S.K.Muzakir, Rebar T.Abdulwahid., Effect of glycerol on EDLC characteristics of chitosan:methylcellulose polymer blend electrolytes, J. Mater. Res. Technol, vol. 9 , pp. 8355–8366, 2020.

[9]E. Chiellini, A. Corti, S. D'Antone, R.Solaro. , Biodegradation of poly (vinyl alcohol) based materials, Progress in Polymer Science , vol. 28 , pp 963-1014, 2003.

[10] X. Lu, M. Yu, G. Wang, Y. Tong, Y. Li,Flexible solid-state supercapacitors: design, fabrication and applications, Energy Environ Sci, vol. 7 , pp 2160–2181, 2014.

[11] S. Alipoori, S. Mazinani, SH Aboutalebi, F. Sharif, Review of PVA-based gel polymer electrolytes in flexible solid-state supercapacitors: Opportunities and challenges, J Energy Storage, 27 (2020)101072.

vol. 27 , pp. 101072 , 2014.

[12] N. Choudhury, S. Sampath, A. Shukla, Hydrogel-polymer electrolytes for electrochemical capacitors, Energy Environ Sci ,vol. 2, pp. 55–67, 2009.

[13] M. S. Mustafa, H. O. Ghareeb, S. B. Aziz, M. A, Brza, S. Al-Zangana, J. M. Hadi, M. F. Z. Kadir, Electrochemical characteristics of glycerolized peo-based polymer electrolytes, Membranes ,vol. 10 , pp.116, 2020.

[14] J. Song , Y. Wang, C. C. Wan, Review of gel-type polymer electrolytes for lithium-ion batteries, J Power Sour, vol. 77 ,pp. 183–197,1999.

[15] S. N. Bhad, V. Sangawar, Synthesis and study of PVA based gel electrolyte, Chem Sci Trans, vol. 1 ,pp. 653–657, 2012.

[16] X. Yang, F.Zhang, L.Zhang, T.Zhang, Y.Huang, Y.Chen , A high-performance graphene oxide-doped ion gel as gel polymer electrolyte for all-solid-state supercapacitor applications, Chem Sci Trans, vol. 23 , pp. 3353–3360 , 2013.

[17] M. Aslam, M. A. Kalyar, Z. A. Raza, Fabrication of nano-CuOloaded PVA composite films with enhanced optomechanical properties, Polym Bull,vol. 78 ,pp. 1551-1571, 2020.

[18] M. Aslam, M. A. Kalyar, Z. A. Raza, Polyvinyl alcohol: a review of research status and use of polyvinyl alcohol based nanocomposites, Polym Eng Sci ,vol. 58, pp. 2119–2132, 2018.

[19] A. Murali, R.Ramesh, M.Sakar, S.J.Park, S.S.Han, Unveiling the potential of emergent nanoscale composite polymer electrolytes for safe and efficient all solid-state lithium-ion batteries , RSC Adv ,vol. 14, pp. 30618-30629, 2024.

[20] M.G. El-Shaarawy, M. Khairy , M.A. Mousa, Structural, electrical and electrochemical properties of ZnO nanoparticles synthesized using dry and

wet chemical methods, Advanc Powder Technol, vol. 31 , pp. 1333–1341, 2020.

[21] G. Prajapati, R. Roshan, P. Gupta, Effect of plasticizer on ionic transport and dielectric properties of PVA–H¬3PO4 proton conducting polymeric electrolytes, vol .71 pp. 1717–1723, 2010.

[22] Y. Pavani, M,Ravi, S.Bhavani, A,Sharma,V.N.Rao., Characterization of poly (vinyl alcohol)/potassium chloride polymer electrolytes for electrochemical cell applications, , J Phys Chem Sol ,vol. 52 ,pp. 168–169, 2012.

[23]V. M. Mohan, V. Raja, A. Sharma, V. N. Rao, Ionic conductivity and discharge characteristics of solid-state battery based on novel polymer electrolyte (PEO+ NaBiF4), vol. 94 , pp. 177–181, 2005.

[24]W.J.Smit,F.Tang,Y.Nagata.M.A.Sanche z,T.Hasegawa,E.H.G.Backusm,M.Bonn, H.J.Bakker, Observation and Identification of a New OH Stretch Vibrational Band at the Surface of Ice, vol. 8 ,pp. 3656–3660, 2017.

[25] D. Ciumac, R. A. Campbell, L. A. Clifton, H. Xu, G. Fragneto, J. R. Lu. Influence of Acyl Chain Saturation on the Membrane-Binding Activity of a Short Antimicrobial Peptide, vol. 2 ,pp. 7482-7492, 2017.

[26] A. Barth, The infrared absorption of amino acid side chains, Progress in Biophysics and Molecular Biology, vol. 74 , pp. 131-173, 2000.

[27] N. Chen, J. h. Zhang, The role of hydrogen-bonding interaction in poly(vinyl alcohol)/poly(acrylic acid) blending solutions and their films, vol. 28 , pp. 903-911, 2010.

[28] G. Prajapati, R, Roshan, P. Gupta, Effect of plasticizer on ionic transport and dielectric properties of PVA–H3PO4 proton conducting polymeric electrolytes, vol .71 , pp.1717–1723, 2010.

[29] B. H. Stuart, Infrared spectroscopy: fundamental and applications, pp. 1-221, ,2004.

[30] S. B. Aziz, R. B. Marif, M. Brza. A, N. Hassan, H. A. Ahmad, Younis, Structural, thermal, morphological and optical properties of PEO filled with biosynthesized Ag nanoparticles: new insights to band gap study, vol. 13 ,pp. 102220, 2019.

[31] C. Zhao, C. Wang, Z. Yue, J. Shu, G. G. Wallace, Intrinsically stretchable supercapacitors composed of polypyrrole electrodes and highly stretchable gel electrolyte, vol. 5 , pp. 9008–9014, 2013.

[32] N. T. B. Linh , K-H Lee, B-T Lee, Fabrication of photocatalytic PVA–TiO¬2 nano-fibrous hybrid membrane using the electro-spinning method, vol. 46 ,pp. 5615–5620, 2011.

[33] R. Zhang, Q. Kuang, H. Cao, S. Liu, X. Chen, X. Wang, F. Wang, Unity Makes Strength: Constructing Polymeric Catalyst for Selective Synthesis of CO2/Epoxide Copolymer, vol. 5 ,pp. 1-26, 2022.

[34] S. B. Aziz, A. Q. Hasssan, S. J. Mohammed, W. O. Karim, M. F. Z. Kadir, H. A. Tajuddin, N. N. M. Y. Chan , Structural and Optical Characteristics of PVA:C-Dot Composites: Tuning the Absorption of Ultra Violet (UV) Region, vol. 9 , pp. 216, 2019.

[35]L. Zhang , Y. Dai, C. Li, Y. Dang, R, Zheng, Z. Wang, Y. Wang, Y. Cui, H. Arandiyan, Z. Shao, H. Sun, Q. Zhuang, Y. Liu, Recent advances in electrochemical impedance spectroscopy for solid-state batteries, vol. 69 , pp. 103378, 2024.

[36] A. S. Marf, S. B. Aziz, R. M. Abdullah, Plasticized H+ ion-conducting PVA:CS-based polymer blend electrolytes for energy storage EDLC application, vol. 31 ,pp. 18554-18568, 2020 .

[37] M. Brza, S. B. Aziz, S. R. Saeed, M. H. Hamsan, S. R. Majid, R. T. Abdulwahid , M. F. Z, Kadir, R. M. Abdullah , Energy Storage Behavior of Lithium-Ion Conducting poly(vinyl alcohol) (PVA): Chitosan(CS)-Based Polymer Blend Electrolyte Membranes: Preparation, Equivalent Circuit Modeling, Ion Transport Parameters, and Dielectric Properties, vol. 10 ,pp. 381, 2020.

[38] B. N. Samartharama, N. Nagaiah, T, Demappa, M. R. Ambika, H. Devendrappa, Investigation on Electrical properties of PEO/CMC solid polymer blend electrolyte, vol. 1221 , pp. 012028, 2022.

[39] A. K. Das, S. Sinha, A. Mukherjee, A.K. Meikap, Enhanced dielectric properties in polyvinyl alcohol – Multiwall carbon nanotube composites, vol. 167 , pp. 286-294, 2015.

[40] I. Latif, B. Taghreed, A. Alwan, H. Al-Dujaili, Low Frequency Dielectric Study of PAPA-PVA-GR Nanocomposites, Nanosci. Nanotech, vol. 2 , pp. 190-200, 2012.

[41]S. K. Shetty, Ismayil, S. Hegde, V. Ravindrachary, G. Sanjeev, R. F. Bhajantri, S. P. Masti, Dielectric relaxations and ion transport study of NaCMC:NaNO3 solid polymer

electrolyte films, vol. 27 ,pp. 2509-2525, 2021.

[42] P. Zaccagnini, L. Baudino, A.Lamberti, A. L. Alexe-Ionescu, G. Barbero, L. R. Evangelista, C. F. Pirri, Electrode polarization in the presence of a first order ionic trapping reaction, vol. 918, pp. 116499,2022.

[43] W. H. Hou, C. Y. Chen, C. C. Wang, Conductivity, DSC, and Solid-State NMR Studies of Comb-Like Polymer Electrolyte with a Chelating Functional Group, vol. 166 ,pp. 397-405 ,2004.

[44] O. Mtioui, H. Litaiem, S. Garcia-Granda, L. Ktari, M. Dammak, Thermal behavior and dielectric and vibrational studies of Cs2(HAsO4)0.32(SO4 0.68Te(OH)6, ,vol. 21, pp. 411–420, 2015.

[45] B.G. Soares, M.E. Leyva, G.M.O. Barra, D. Khastgir, Dielectric behavior of polyaniline synthesized by different techniques, vol. 42 , pp. 676-686, 2006.

[46] B. Chatterjee, P. N. Gupta, Nanocomposite films dispersed with silica nanoparticles extracted from earthworm humus, vol 358 ,pp 3355–3364,2012.

[47] A. S. F. M. Asnawi, S. B. Aziz, M. M. Nofal, M. H. Hamsan ,M. A. Brza, Y. M. Yusof, R. T. Abdilwahid, S. K. Muzakir, M. F. Z. Kadir , Glycerolized Li+ Ion conducting chitosan-based polymer electrolyte for energy storage EDLC device applications with relatively high energy density, Polymers, vol. 12 , pp. 1433, 2020.

[48] A. Pawlicka, F.C.Tavares, D.S.Dorr, C.M.Cholant, F.Ely, M.J.L.Santos, C.O.Avellaneda, Dielectric behavior and FTIR studies of xanthan gum-based solid polymer electrolytes,vol. 305 ,pp. 232–239,2019.

[49] F. Tian, Y. Ohki, Electric Modulus Powerful Tool for Analyzing Dielectric Behavior, IEEE Transactions on Dielectrics and Electrical Insulation, vol. 21, pp. 929, 2014.